Raman scattering from small spherical particles

Maurizio Montagna
Istituto Nazionale di Fisica della Materia, Dipartimento di Fisica, Universitá di Trento, I-38050 Povo, Trento, Italy

Roberto Dusi
Institut für Theoretische Physik III, Universität Stuttgart, Pfaffenwaldring 57, 70550 Stuttgart, Germany
(Received 5 April 1995; revised manuscript received 6 July 1995)

Raman coupling coefficients are calculated for the acoustic vibrations of a small dielectric sphere. The mean components of the strain tensor are calculated for the symmetric and quadrupolar Raman-active vibrational modes, within a continuum approximation which considers a vibrating homogeneous sphere. The Raman coupling coefficient depends on the crystalline structure and on the microscopic scattering mechanism. For cubic Bravais lattices and for a dipole-induced dipole scattering mechanism, the coupling coefficient of the symmetric vibrations vanishes. The Raman intensity of the inner modes is found to be small with respect to that of surface modes. The scaling law, which gives the Raman coupling coefficient as a function of the particle size, has been derived. The coupling of the sphere with a surrounding elastic medium has been considered and found to cause shift and broadening of the lines. These effects can alter significantly the estimated mean value and distribution of particle sizes.

I. INTRODUCTION

Glasses containing metallic or semiconductor clusters with a size of a few nanometers are of high interest for nonlinear optics applications.[1] Three-dimensional quantum size effects enhance the nonlinear response of the glass by several orders of magnitude. The nonlinear properties are connected to the size of the clusters.

After the first works on rough metal surfaces,[2] on spinel nanocrystals in cordierite glasses,[3] and on silver colloids in alkali halides,[4,5] low-frequency Raman scattering from symmetric and quadrupolar acoustic vibrations of the spheroidal clusters has become a method to determine the size of the particles. A peak in the range 5–50 cm^{-1} was observed in many composite systems containing metallic, insulator, or semiconductor nanoparticles.[3,5–14] The size of the nanoparticles was deduced from the energy of the peak, since the frequency of all modes scales as the inverse of the linear dimension of the particle. In most studies a spherical shape was assumed for the particles, and the peaks in the Raman spectra were indeed assigned to the acoustic vibrations of a free sphere. The vibrational eigenfrequencies and eigenvectors of a homogeneous elastic sphere with a free surface were studied by Lamb.[15] The vibrations are grouped into two categories, the torsional ones and the spheroidal ones. The former involve only shear motions and do not change the volume of the sphere, the latter involve both shear and stretching motions and produce radial displacement. Torsional and spheroidal modes are classified according to the symmetry group of the sphere by the labels (l,m) as for the spherical harmonic functions Y_l^m. The symmetric $l=0$ spheroidal modes are purely radial with spherical symmetry. At higher l values, angular corrugation appears: l measures the number of wavelengths along a circle on the surface.[16] A third index $(p=0,1,...,n)$ labels the sequence of eigenmodes, in increasing order of frequency and radial wave vector, at fixed angular shape (l,m). Mode counting is achieved by fixing limits to l and p: one can use the continuum approximation, but one must remember that in a sphere containing N atoms there are $3N-6$ vibrational modes.[16]

Recently, Duval[17] has shown, on the basis of symmetry arguments, that the only Raman-active modes of a sphere are the symmetric $l=0$ and quadrupolar $l=2$ spheroidal modes. The former produce polarized and the latter depolarized spectra. Therefore, on the basis of the depolarization ratio I_{HV}/I_{VV}, one should be able to assign the Raman spectra to symmetrical or quadrupolar vibration.

Silver particles in alkali halides,[5,7] have depolarized spectra, which were indeed assigned to quadrupolar vibrations. In particular, Mariotto *et al.*[5] found that the particles were ellipsoidal, and the degeneracy of the $l=2$ quadrupolar modes was lifted. The energies and relative intensities of the three peaks observed in VV and HV polarizations were very well reproduced by considering the lifting of the degeneracy of the $m=0$, ±1, ±2 components. Depolarized spectra were also obtained for silver particles in silica.[12,18] Fujii *et al.*[12] reported on a depolarization ratio I_{VH}/I_{VV} of 0.27 and assigned the line to $l=2$ spheroidal modes. On the other hand, the $l=0$ spheroidal modes seem to dominate the Raman spectra of nanocrystalline particles of CdS in glasses:[13,14] all structures are polarized, apart from one peak in the smallest particles, which was indeed attributed to $l=2$ modes.[13] Similar arguments led Capobianco *et al.* to conclude that nanocrystals nucleated in aluminosilicate glasses by Eu^{3+} or by Cr^{3+} ions, acting as nucleating centers, give low-frequency Raman scattering due to $l=2$

0163-1829/95/52(14)/10080(10)/$06.00

and $l = 0$ spheroidal modes, respectively.[11]

At present, it is not clear why the $l = 0$ modes should dominate in some systems and the $l = 2$ modes in others. Furthermore, it would be interesting to know the relative importance in the Raman spectra of modes with definite l values but with different p values. So far, the structures observed in Raman spectra were attributed, both for $l = 0$ and 2, to the $p = 0$ fundamental mode, also called the surface mode. To our knowledge, only in one case[13] were the observed peaks assigned to inner modes with $p = 1$.

Another important question is the dependence of the Raman coupling coefficient on the size of the particles. This function is necessary to obtain the size distribution of the particles from the experimental line shape. Also necessary to this aim is the knowledge of the homogeneous line shape. In fact, a free sphere has a discrete set of vibrational modes, but when the sphere is embedded in an elastic medium, the discrete set broadens into a continuum.

In this work we study the following: (1) The relative scattering efficiency in VV and HV polarizations of the two sets of Raman active modes, the $l = 0$ and 2 spheroidal vibrations. (2) The relative scattering efficiency of the higher harmonics (inner modes) with respect to their fundamental modes (surface modes). (3) The scaling law, i.e., the scattering efficiency as a function of the particle size. (4) The effect of a surrounding elastic medium that causes shift and broadening of the lines.

We will begin by studying the problem for one-dimensional systems. This is interesting in itself and helps in discussing the methods used in the calculations and the limits of application of the results.

II. RAMAN SCATTERING

The spectral density of the scattered light is given by[19]

$$I_{\alpha\beta}(\mathbf{q},\omega) \propto \int dt e^{-i\omega t}\langle \delta\epsilon^*_{\alpha\beta}(\mathbf{q},0)\delta\epsilon_{\alpha\beta}(\mathbf{q},t)\rangle, \quad (1)$$

where α and β are the direction of polarization of the incident and scattered photon; $\hbar\omega = \hbar\omega_i - \hbar\omega_s$ and $\mathbf{q} = \mathbf{k}_i - \mathbf{k}_s$ are the exchanged energy and wave vector. The fluctuations of the dielectric constant can be described in terms of the space Fourier transform of the macroscopic polarizability density tensor $P_{\alpha\beta}(\mathbf{r},t)$

$$\delta\epsilon_{\alpha\beta}(\mathbf{q},t) \propto \int d\mathbf{r} e^{-i\mathbf{q}\cdot\mathbf{r}(t)} P_{\alpha\beta}\mathbf{r},t)$$

$$= \sum_i e^{-i\mathbf{q}\cdot\mathbf{r}^i(t)}\pi^i_{\alpha\beta}(t), \quad (2)$$

which in atomic or molecular systems can be described microscopically by using the effective microscopic polarizability tensor $\pi^i_{\alpha\beta}(t)$ of the ith scatterer at position $\mathbf{r}^i(t)$

$$\mathbf{r}^i(t) = \mathbf{x}^i + \mathbf{u}^i(t), \quad (3)$$

where $\mathbf{u}^i(t)$ is the displacement from the equilibrium position $\mathbf{x}^i$. Since we are interested only in Raman scattering from systems with size (R) small compared with the wavelength of the light ($qR \ll 1$), and not in the Brillouin scattering, we can consider $\mathbf{q} = 0$. $\pi^i_{\alpha\beta}(t)$ can be expanded in power series of the displacements $\mathbf{u}^j$, and $\mathbf{u}^i$ can be expressed in terms of the vibrational eigenvectors $\mathbf{e}(i,p)$, whose frequencies are ω_p. The contribution of the pth mode to the Stokes part of the spectrum can be put in the form:[20]

$$I_{\alpha\beta}(\omega_p) \propto \frac{n(\omega_p)+1}{\omega_p}\left|\sum_{ij}\sum_\gamma \frac{\partial\pi^i_{\alpha\beta}}{\partial u^j_\gamma}[e_\gamma(j,p) - e_\gamma(i,p)]\right|^2$$

$$= \frac{n(\omega_p)+1}{\omega_p} C_{\alpha\beta}(\omega_p) \quad (4)$$

where $n(\omega,T)$ is the Bose-Einstein factor and $C_{\alpha\beta}(\omega_p)$ is the mode-radiation coupling coefficient.

III. LINEAR CHAIN

Consider a linear chain of N equal masses, M, placed at rest distance a, linked by harmonic springs. The masses have longitudinal motions along the chain. The rest length of the chain is $L = (N-1)a$. For free boundary conditions the eigenvectors are

$$e(i,p) = \sqrt{\frac{2}{N}}\cos(k_p x_i), \quad (5)$$

where $k_p = \frac{\pi p}{L}$, $1 \le p \le N-1$. In this case the Raman coupling coefficient becomes

$$C(p) = \left|\sum_{ij} A_{ij}[e(j,p) - e(i,p)]\right|^2. \quad (6)$$

The quantities $A_{ij} = \frac{\partial\pi^i}{\partial u^j}$ depend on the scattering mechanism. In the bond polarizability (BP) model $A_{ij} = A_1(\delta_{j,i+1} - \delta_{j,i-1})$ and the coupling coefficient is

$$C^{\mathrm{BP}}(p) = A_1^2\left|\sum_i e(i+1,p) - e(i,p)\right|^2$$

$$= A_1^2\left|e(N,p) - e(1,p)\right|^2 = \frac{8}{N}A_1^2 \quad (7)$$

for odd values of p, while $C^{\mathrm{BP}}(p) = 0$ for even values of p. Let us discuss the physical origin of Eq. (6), i.e., C=const. In a BP model, where the polarizability of the bonds varies linearly with the bond length, the modulation of polarizability of the whole chain, to be considered as a molecule for $L \ll \lambda_{\mathrm{light}}$, is proportional to the modulation of the length of the chain, $e(N,p) - e(1,p)$, produced by the mode p. In a continuum approximation, valid for long vibrational wavelengths ($k_p a \ll 1$), the eigenvectors are given by

$$e_p(x) = \sqrt{\frac{2}{L}} \cos(k_p x), \tag{8}$$

whose eigenfrequencies are $\omega_p = v k_p$, where v is the (longitudinal) sound velocity. The Raman coupling coefficient can be calculated in terms of the contributions of the modes to the local strain:

$$C_p \propto \left| \int \frac{\partial e_p(x)}{\partial x} dx \right|^2 = | e_p(L) - e_p(0) |^2 . \tag{9}$$

All modes with odd p, i.e., the symmetric modes which modulate the length of the chain, have the same Raman coupling coefficient, even if the local strain increases linearly with k_p. This is so because the scattered waves, whose amplitude increases with k_p, undergo destructive interference: half a vibrational wavelength, for odd p, contributes because the contributions of the others wavelengths cancel each other. Even if all Raman active modes have the same coupling coefficient, the Raman intensity of the first mode ($p = 1$) will be higher than that of the other odd harmonics due to the factor $(n+1)/\omega \simeq K_B T/\omega^2$ for $K_B T \gg \hbar\omega$. Therefore, in the Raman spectrum of the linear chain, we expect a mode at $\omega_1 = \pi v/L$ and the odd harmonic at $\omega = 3\omega_1, 5\omega_1, \ldots$ with intensity decreasing as ω^{-2}.

From Eq. (8) we obtain the scaling law for $C(\omega)$; comparing chains of different lengths, for any mode and in particular for the first one we have

$$C(\omega_1) \propto \frac{1}{L} \propto \omega_1. \tag{10}$$

Therefore, the Raman intensity, in the high-temperature limit ($K_B T \gg \hbar\omega_1$) scales as

$$I(\omega_1) = C(\omega_1) \frac{n+1}{\omega_1} \simeq \frac{1}{\omega_1} \simeq L. \tag{11}$$

In the presence of a distribution of different chains, the Raman activity of any mode is proportional to the length of the chains.

In a dipole-induced dipole (DID) mechanism of light scattering we have[21]

$$\left(\frac{\partial \pi^i_{\alpha\beta}}{\partial u^i_\gamma} \right)^{\mathrm{DID}} = \frac{2\alpha^2}{a^4} T^{(3)}_{\alpha\beta\gamma}(\mathbf{x}^{ij}), \tag{12}$$

where α is the bare polarizability of the elementary scatterers, $\mathbf{x}^{ij} = \mathbf{x}^j - \mathbf{x}^i$ is the equilibrium distances of the pair of scattering units i, j and $T^{(3)}_{\alpha\beta\gamma}(\mathbf{r}) = -[\nabla_\alpha \nabla_\beta \nabla_\gamma (\frac{1}{|\mathbf{r}|})]$. The strong spatial dependence of the dipole operators gives, for the linear chain, DID results very similar to those of BP, which can be obtained formally by limiting the sums in the DID expression to nearest-neighbor elementary scatterers.[21]

IV. THE SPHERE

Passing to three dimensions, we are faced with the problem that the vibrational dynamics is easily described in a continuum approximation, but the scattering depends on the microscopic details of the discrete structure. Within a DID model the quantities of interest are

$$B^p_{\alpha\beta} = (C^p_{\alpha\beta})^{\frac{1}{2}} \propto \sum_\gamma \sum_{ij} T_{\alpha\beta\gamma}(\mathbf{x}^{ij}_\gamma)[e_\gamma(\mathbf{x}^j, p) - e_\gamma(\mathbf{x}^i, p)]. \tag{13}$$

In a continuum approximation we expand the relative displacements of the scatterers,

$$e_\gamma(\mathbf{x}^j, p) - e_\gamma(\mathbf{x}^i, p) = \sum_\delta \frac{\partial e_\gamma(\mathbf{x}^i, p)}{\partial x_\delta} \mathbf{x}^{ij}_\delta, \tag{14}$$

obtaining

$$B^p_{\alpha\beta} = \sum_{\gamma\delta} \sum_i A_{\alpha\beta\gamma\delta}(\mathbf{x}^i) \frac{\partial e_\gamma(\mathbf{x}^i, p)}{\partial x_\delta}, \tag{15}$$

where

$$A_{\alpha\beta\gamma\delta}(\mathbf{x}^i) = \sum_j T_{\alpha\beta\gamma}(\mathbf{x}^{ij}) x^{ij}_\delta. \tag{16}$$

Equation (16) becomes simpler if the quantities $A_{\alpha\beta\gamma\delta}(\mathbf{x}^i)$ are not site dependent. Though this is in principle true only for infinite crystalline systems, we assume that it holds also for our systems and obtain

$$B^p_{\alpha\beta} = \sum_{\gamma\delta} A_{\alpha\beta\gamma\delta} \sum_i \frac{\partial e_\gamma(\mathbf{x}^i, p)}{\partial x_\delta} = \sum_{\gamma\delta} A_{\alpha\beta\gamma\delta} \int \frac{\partial e_\gamma(\mathbf{x}, p)}{\partial x_\delta} dv, \tag{17}$$

where the sum on the point scatterers is converted into an integral on the volume of the sphere.

This solves our problem: $A_{\alpha\beta\gamma\delta}$ are quantities that depend on the microscopic structure and on the scattering mechanism (DID or BP) but not on the dynamics; the vibrational dynamics will be treated in a continuum approximation. For each mode of the sphere, we need the components of the local strain averaged over the volume of the sphere:

$$\int \epsilon_{\alpha\beta} dv = \langle \epsilon_{\alpha\beta} \rangle \frac{4\pi}{3} R^3. \tag{18}$$

Actually the local strain is defined as

$$\epsilon_{\alpha\beta} = \frac{1}{2} \left(\frac{\partial e_\alpha}{\partial x_\beta} + \frac{\partial e_\beta}{\partial x_\alpha} \right), \tag{19}$$

but it can be shown that, by averaging over the volume of the sphere, $\langle \frac{\partial e_\alpha}{\partial x_\beta} \rangle = \langle \frac{\partial e_\beta}{\partial x_\alpha} \rangle$.

As mentioned, a sphere has two types of vibrational modes, spheroidal ones and torsional ones, but the latter are not Raman active.[17] Spheroidal modes involve both stretching and shear motions and can be described in terms of a scalar and a vector potential.[15,16,22–24] Following Love,[22] the components of the normalized eigenvectors $\bar{e}(\bar{r})$ are given by

$$e_\alpha^{plm} = A\left[-\frac{1}{h^2}\left(\Psi_l(hr)+\frac{hr}{2l+1}\Psi_l'(hr)\right)\frac{\partial Q_l}{\partial x_\alpha}+\frac{1}{(2l+1)h}\Psi_l'(hr)r^{2l+2}\frac{\partial}{\partial x_\alpha}\left(\frac{Q_l}{r^{2l+1}}\right)\right.$$
$$\left.+\Psi_{l-1}(kr)\frac{\partial b_l}{\partial x_\alpha}-\frac{l}{l+1}\Psi_{l+1}(kr)k^2r^{2l+3}\frac{\partial}{\partial x_\alpha}\left(\frac{b_l}{r^{2l+1}}\right)\right] \quad (20)$$

where x_α and e_α are the Cartesian components of the position and of the normalized displacements, respectively. The modes are classified according to the angular indexes l,m. $Q_l = a_{pl}r^lY_{l,m}(\theta,\phi)$ and $b_l = b_{pl}r^lY_{l,m}(\theta,\phi)$ are the potentials with the symmetry of the spherical harmonics. The ratio a_{pl}/b_{pl} is given by the stress-free boundary conditions. The functions $\Psi_l(hr)$, $\Psi_l(kr)$ are related to the Bessel functions by the relations $\Psi_l(hr) = (-\frac{1}{hr})^l j_l(hr)$; $\Psi'(x) = \frac{d\Psi}{dx}$. h and k are analogous to the wave vectors of longitudinal and transverse phonons and are connected to the frequency of the modes by the relations $\omega = hV_L = kV_T$, where V_L and V_T are the longitudinal and transverse sound velocities. The index $p = 1,2,...$ labels the sequence of solutions with fixed l,m in increasing order of energy. These solutions for h_p and $k_p = h_pV_L/V_T$ are given by the stress-free boundary conditions. To calculate the Raman coupling coefficient we need normalized vibrational modes:

$$\int |\mathbf{e}|^2 dv = 1. \quad (21)$$

This fixes the value of the constant A in Eq. (20). Taking the derivative of Eq. (20), we obtain

$$\frac{\partial e_\alpha^{plm}}{\partial x_\beta} = [A(r)x_\alpha x_\beta + B(r)\delta_{\alpha,\beta}]r^lY_{lm}(\theta,\phi)$$
$$+C(r)x_\beta\frac{\partial r^lY_{lm}(\theta,\phi)}{\partial x_\alpha}+D(r)x_\alpha\frac{\partial r^lY_{lm}(\theta,\phi)}{\partial x_\beta}$$
$$+E(r)\frac{\partial[2r^lY_{lm}(\theta,\phi)]}{\partial x_\alpha\partial x_\beta}, \quad (22)$$

where $A,B,C,...$ are radial functions typical of each mode with frequency ω_{pl}.

From Eq. (22), and from the orthogonality properties of spherical harmonics, it results that only for the $l = 0$ and 2 modes the integral of the strain is different from zero. This is easily seen by noting that x_α have the same angular dependence as Y_1, $x_\alpha x_\beta$ as a linear combination of Y_0 and Y_2, and that the space derivative of the quantities r^lY_l transform as $r^{l-1}Y_{l-1}$.

The values of the mean strain in Eq. (18) can be calculated for all p,l,m using Eq. (22) and depend on the radius of the sphere R and on the values of the sound velocity V_L, V_T. Actually one can calculate only the mean strain $\langle\epsilon_{zz}\rangle$ for the $l = 0$ and $l = 2, m = 0$ modes and then use symmetry considerations that give the results of Table I, where we report $\langle\epsilon_{\alpha\beta}\rangle$ for the spheroidal $l = 2, m$ modes. $\langle\epsilon_{zz}\rangle$ for the $l = 0$ and for the $l = 2, m = 0$ modes have been numerically calculated by Eq. (22) for a few low-p values and for $V_L/V_T = \sqrt{3}$, which corresponds to the Poisson condition $\lambda = \mu$, where λ and μ are the Lame' constants. In Table II we report the squared values. The other $\langle\epsilon_{\alpha\beta}\rangle$ can be obtained from Table I.

Now we can calculate the Raman coupling coefficients by using Eq. (15), provided we know the $A_{\alpha\beta\gamma\delta}$ coefficients, which depend on the microscopic structure and scattering mechanism. The $A_{\alpha\beta\gamma\delta}$ values for a given structure will determine the relative importance of the $l = 0$ and 2 modes in the Raman spectra. The simplest example is DID in a cubic Bravais lattice. In this case, the nonzero $A_{\alpha\beta\gamma\delta}$ are[25]

$$A_{\alpha\alpha\alpha\alpha} = -2s, \quad (23)$$
$$A_{\alpha\alpha\beta\beta} = A_{\alpha\beta\alpha\beta} = A_{\alpha\beta\beta\alpha} = s\ (\alpha\neq\beta), \quad (24)$$

where s is a constant, which depends on the structure.

By using in Eq. (15) the values of Table I for the mean strains, we find for the spheroidal $l = 0$ mode $B_{xx} = B_{yy} = B_{zz} = 0$: the $l = 0$ mode is not Raman active in nanoparticles with cubic Bravais lattice and for the DID scattering mechanism. This result could explain why the $l = 2$ mode dominates the Raman spectra of silver nanoparticles.

For the $l = 2$ spheroidal mode, by averaging over the five m components and over the directions of polarization [$I_{VV} = \frac{1}{3}(I_{xx}+I_{yy}+I_{zz})$, $I_{HV} = \frac{1}{3}(I_{xy}+I_{yz}+I_{zx})$], we obtain a depolarization factor $I_{HV}/I_{VV} = 1/3$. This ratio is in quite good agreement with the few available experimental results for the scattering due to $l = 2$ modes. Fujii *et al.*[12] found $I_{HV}/I_{VV} \simeq 0.27$ for Ag particles in silica glass and Abel[7] found $I_{HV}/I_{VV} \simeq 1/3$ for Ag particles in KBr crystals.

The Raman intensities of the inner modes with respect to the surface ones are given in Table II. All coupling coefficients, that are proportional to the square of the

TABLE I. Relative values of the components of the strain, averaged over the sphere, for the m components of the $l = 2$ spheroidal mode.

m	xx	yy	zz	xy	yz	zx
±2	$\frac{\sqrt{3}}{\sqrt{2}}$	$-\frac{\sqrt{3}}{\sqrt{2}}$	0	$\pm i\frac{\sqrt{3}}{\sqrt{2}}$	0	0
±1	0	0	0	0	$\pm i\frac{\sqrt{3}}{\sqrt{2}}$	$\frac{\sqrt{3}}{\sqrt{2}}$
0	-1	-1	2	0	0	0

TABLE II. Adimensional frequencies ($kR = \omega R/V_T$, $hR = \omega R/V_L$) for the surface modes ($p = 1$) and the first inner modes ($2 \leq p \leq 5$) of the $l = 0$ and $l = 2$, $m = 0$ spheroidal modes; squares of the $\langle \epsilon_{zz} \rangle$ (see text); Raman intensity of the inner modes normalized to those of the surface ones.

	p	kR	hR	$\lvert\langle \epsilon_{zz} \rangle\rvert^2$	I
	1	4.43	2.56	4.22	1
	2	10.49	6.06	2.97	0.12
$l = 0$	3	16.07	9.27	2.86	0.047
	4	21.6	12.5	2.83	0.028
	5	27.05	15.61	2.81	0.018
	1	2.64	1.52	7.2	1
$l = 2$	2	4.86	2.81	0.54	0.022
	3	8.33	4.81	1.01	0.014
$m = 0$	4	9.78	5.65	2.45	0.025
	5	12.16	7.02	2.79	0.018

averaged strain, have comparable values, a result similar to that of the linear chain: the local strains increase with the radial wave vector, and indeed with frequency, but their mean values on the sphere, which are proportional to the amplitude of the scattered wave, present cancellation effects. However, the surface modes dominate the spectra because of the $(n + 1)/\omega \simeq K_B T/\omega^2$ factor in the intensity of the scattering, as can be seen in the last column of Table II.

The scaling law, which provides the dependence of the Raman coupling coefficient on the radius R of the particles, can be deduced from Eq. (22), by taking into account the mode normalization [Eq. (21)]. For any mode (l, m, p) the frequency scales as the inverse of the radius of the sphere ($\omega \propto 1/R$), the normalized displacements at the normalized position $\mathbf{r}/R$ scale as the square root of the inverse volume [$\mathbf{e}(\mathbf{r}/R) \propto R^{-\frac{3}{2}}$], the local strains scale as e/R ($\frac{\partial e}{\partial x} \propto R^{-\frac{5}{2}}$), and the integral of the strain in Eq. (18) scales as the local strain times the volume of the sphere ($R^{\frac{1}{2}}$). Therefore, the scaling law for the coupling coefficient is given by

$$C(\omega) \propto R \propto \frac{1}{\omega}. \tag{25}$$

Taking into account the $(n+1)/\omega \simeq K_B T/\omega^2$ factor, the intensity is found to scale as

$$I(\omega) \propto \omega^{-3} \propto R^3. \tag{26}$$

Spheres of different sizes contribute to the Raman scattering proportionally to their volume for any allowed vibrational mode.

Finally, in Fig. 1 we show the frequencies of the quadrupolar and symmetric surface modes of a free vibrating sphere, as a function of the ratio of the longitudinal and transverse sound velocities. For graphical reasons, we show the quantities kR for the quadrupolar $l = 2$ mode and hR for the symmetrical $l = 0$ mode. The frequency of the modes are given by $\omega_2 = (kR)V_T/R$ and $\omega_0 = (hR)V_L/R$.

V. NONSPHERICAL PARTICLES

The results obtained in Sec. IV were for a free spherical particle. It is interesting to discuss, at least qualitatively, what is expected in real systems when the particle does not have spherical symmetry and is embedded in an elastic medium. Let us first discuss the effect of a symmetry lowering. The free vibrations of the sphere are labeled with the angular numbers l, m and the radial number p. All mode frequencies will be affected by a lowering of the spherical symmetry but to different degrees. The lowest modes will be very similar to those of a spherical particle, and we can use for them the labeling of the spherical symmetry. The frequency of the spherical $l = 0$ mode will be related to a mean diameter of the particles, and small protrusions on the surface of the particles will have no important effects on it. For the $l = 2$ spherical

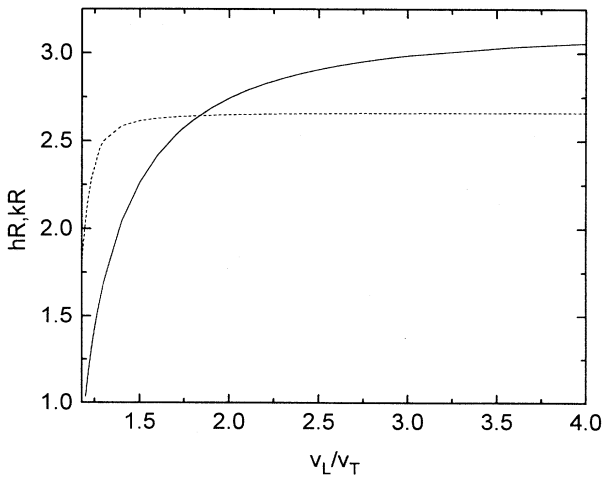

FIG. 1. Adimensional frequencies of the surface modes of a free sphere as a function of the ratio between the longitudinal and transverse sound velocities V_L/V_T. Solid line: $hR = \omega_0 R/V_L$ for the symmetric $l = 0$ mode; dashed line: $kR = \omega_2 R/V_T$ for the quadrupolar $l = 2$ mode.

modes we will approximate the particle as an ellipsoid: the modes with $m = 0, \pm 1, \pm 2$ are no longer degenerate and the splittings depend on the eccentricity.[16] At higher l values, protrusions on the surface with a small radius of curvature become more and more important. The simple rules for spherical symmetry, i.e., Raman activity of the $l = 0$ and 2 spheroidal modes and much higher intensity from the surface mode with respect to inner modes, will be partially relaxed. In fact, a surface protrusion with a given radius of curvature tends to vibrate according to modes that, as regard energy and wave function, are similiar to the modes of a sphere with that curvature. Therefore, we expect that the Raman spectrum of a nonspherical particle will contain contributions from all modes: the relative Raman activity of the high-frequency modes with respect to the symmetric and quadrupolar surface modes, will depend on the details of the shape of the particle. For example, Na colloids in a NaCl crystal[26] show a continuous Raman spectrum. This is interpreted by a continuum distribution of radii of curvature of the surface, which has a fractal structure as shown by small-angle x-ray scattering.[27] However, in nearly spherical particles, we expect that the results of the preceding section hold, but with some enhancement of the Raman activity of the high-frequency harmonics.

Recently, Ferrari *et al.* have observed Raman peaks with important high-frequency tails in films of silica containing Ag nanoparticles.[18] The tail is attributed to the deviation from spherical shape; the relative importance of the tail decreases after laser annealing, which increases the size and smooths the surface of the particles. However, only a few experiments have been done on this subject; Raman measurements on nanoparticles with well-defined shape would be very interesting.

VI. MATRIX EFFECT

The results for free particles were obtained assuming stress-free boundary conditions. In the presence of an external medium the new boundary conditions consist in requiring the continuity of the vibrational displacements and of the stress at the interface. The acoustic phonons of the medium are refracted and reflected at the interface, and the important parameters are the ratios of densities and sound velocities. The resulting stationary waves will have the symmetry of the particle. All low-frequency acoustic vibrations involve the whole systems, the particle and the surrounding medium. To follow the evolution resulting from the discrete spectrum of the free particle to the continuum one, a useful quantity is the projected density of states (PDOS), defined as the mean-square displacement of modes at frequency ω within the particle. We will discuss first the one-dimensional problem, which is very simple and provides the same qualitative results of the more complicated three-dimensional case.

A. Linear chain

We consider the longitudinal acoustic modes of a segment of length L with linear mass density ρ and longitudinal sound velocity V_L embedded in an infinite medium with density ρ_m and velocity V_{Lm}. Taking the origin at the center of the segment, the symmetric Raman-active mode with frequency ω is given by

$$e(x,\omega) = A(\omega)\sin(kx), \quad |x| \le L/2, \tag{27}$$

$$e_m(x,\omega) = A_m(\omega)\sin(k_m x) + B_m(\omega)\cos(k_m x), \quad |x| \ge L/2$$

with the condition $\omega = kV_L = k_m V_{Lm}$. The boundary conditions are given by the continuity of the displacement $e(x,\omega)$ and of the stress $\rho V_L^2 \partial e(x,\omega)/\partial x$ at the interface ($|x| = L/2$). The presence of the finite segment has negligible effects on the density of states (DOS) of the composite system, which is the same as that of the infinite medium, i.e., a constant DOS in the low-frequency, nondispersive part of the spectrum. This is achieved by the condition $A_m^2(\omega) + B_m^2(\omega) =$const. With this condition, we obtain

$$A(\omega) \simeq \left\{ \left[\sin\left(\frac{kL}{2}\right) \right]^2 + \left(\frac{\rho V_L}{\rho_m V_{Lm}} \right)^2 \cos(kL/2)^2 \right\}^{-1/2} \tag{28}$$

and can thus calculate the PDOS and the Raman spectra. In Fig. 2 these quantities are reported for some values of the parameter $\alpha = \frac{\rho V_L}{\rho_m V_{Lm}}$. For $\alpha \gg 1$, the PDOS shows sharp peaks, at the frequencies of the sequence

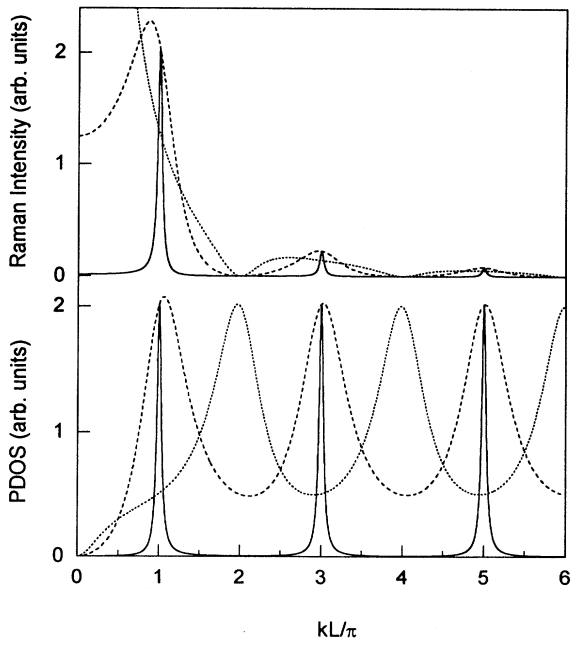

FIG. 2. Projected density of states and Raman intensity of the longitudinal acoustic modes of a segment of length L with linear density ρ and longitudinal sound velocity V_L, embedded in a medium with ρ_m and $V_{Lm} = V_L$. Solid lines: $\rho_m/\rho = 0.05$; dashed lines: $\rho_m/\rho = 0.5$; dotted lines: $\rho_m/\rho = 2$.

$$\omega = V_L k_p, \quad k_p = \frac{\pi}{L} p, \quad p = 1, 3, 5, ..., \tag{29}$$

since this case approaches the free boundary conditions. As α decreases and approaches the value $\alpha = 1$ the peaks in the PDOS become increasingly broad and shift towards high energy. This is especially true for the first peak.

As in Eq. (9), the Raman coupling coefficient $C(\omega)$ of the mode with frequency ω is proportional to the squared amplitude of the modulation of the segment length caused by that mode. The upper part of Fig. 2 shows the high-T Raman spectra:

$$I(\omega) = C(\omega)\frac{n+1}{\omega} \propto \frac{C(\omega)}{\omega^2} T. \tag{30}$$

The zeros of the Raman spectra are for $\omega = V_L k_n = V_L(2\pi/L)n$ $(n = 1, 2, ...)$, i.e., for vibrations with nodes at the boundaries. The $1/\omega^2$ term shifts the Raman peaks towards low energy. The lowest-energy peak extends down to $\omega = 0$ with finite intensity. The case $\alpha < 1$(dotted line in Fig. 2) is more similar to fixed boundary conditions ($\alpha = 0$) than to free boundary conditions ($\alpha = \infty$), and the maxima of the PDOS are for modes that have nodes near to the boundary. However, these modes have very low Raman activity, and therefore the Raman spectrum consists of broad bands without any correlation with the shape of the PDOS. Strong Raman scattering occurs at low frequency with a shape that is a zero-centered Lorentzian with a width at half maximum

$$\frac{\Gamma}{2} = \frac{2\alpha V}{L} = \frac{2\rho V}{\rho_m V_m}\frac{V}{L}, \tag{31}$$

as can be seen from Eq. (28) in the limit of $k = \omega/V_L \to 0$. Figure 2, upper part, shows only the tail of the Lorentzian, which reaches a maximum of about 6 at $\omega = 0$. We will see that this "quasielastic" scattering is not present in the three-dimensional case.

B. The sphere

The matrix effects on the spheroidal modes of the sphere can be calculated as for the segment by considering the continuity of the components of the displacement and of the stress at the interface. The $l = 0$ symmetric modes are simpler to calculate because they involve only radial displacement and stress, i.e., the σ_{rr} component of the stress tensor. As in the one-dimensional case, the "infinite spherical" surrounding medium has a constant density of states for fixed l and m; the ω^2 dependence of the low-frequency acoustic modes is assured by the sum over the different l, m values. In the one-dimensional case, longitudinal and transverse vibrations have a separate nature, and thus a single parameter, $\alpha = \frac{\rho V}{\rho_m V_m}$, is needed. On the other hand, spherical modes are neither transverse nor longitudinal, and as a consequence the parameters ρ_m/ρ, V_{Lm}/V_L, V_L/V_T, V_{Lm}/V_{Tm} are independent. In Fig. 3 we show the behavior of the $l = 0$ symmetric spectrum for $V_L/V_{Lm} = 1$, $V_L/V_T = V_{Lm}/V_{Tm} = \sqrt{3}$, and for some values of the parameter ρ_m/ρ. For $\rho_m/\rho = 0.02$ we obtain sharp peaks with frequencies and intensities close to those of the free sphere of Table II. By increasing ρ_m/ρ the lines broaden and shift in a way similar to that observed for the one-dimensional case, but here the intensity goes to zero at low frequency. Figure 3 also shows the Raman spectrum for $\rho_m = \rho$ (dotted line). In this case all mechanical parameters, densities, and sound velocities are the same for the sphere and for the surrounding medium. Actually, Raman scattering also occurs in this case if a mismatch of the acousto-optical properties of the particle and medium is present.

We will discuss in some detail this limiting problem. In this case, to describe the vibrations of the composite system we do not need to work in spherical symmetry. The low-frequency acoustic modes are phonons with defined wave vector and longitudinal or transverse polarization, which travel in the composite system without any refraction or reflection at the interface. Consider a phonon with wave vector $\bar{k}$, given by

$$\mathbf{e} = \frac{\mathbf{e}_0 e^{i\mathbf{k}\cdot\mathbf{r}}}{\sqrt{V}}. \tag{32}$$

In this case, Eqs. (15) and (17) give

$$B^{\mathbf{k}}_{\alpha\beta} = \frac{i}{\sqrt{V}} \sum_{\gamma\delta} e_{0\gamma} k_\delta \int_V A_{\alpha\beta\gamma\delta} e^{i\mathbf{k}\cdot\mathbf{r}} dv. \tag{33}$$

Under the assumption that $A(\mathbf{r})$ has two constant values A^s for the sphere and A^m for the medium, with a mismatch $\Delta A = A^s - A^m$, we have

$$B^{\mathbf{k}}_{\alpha\beta} = \frac{i}{\sqrt{V}} \sum_{\gamma\delta} e_{0\gamma} k_\delta \Delta A_{\alpha\beta\gamma\delta} \int_{\text{sphere}} e^{i\mathbf{k}\cdot\mathbf{r}} dv, \tag{34}$$

since the term

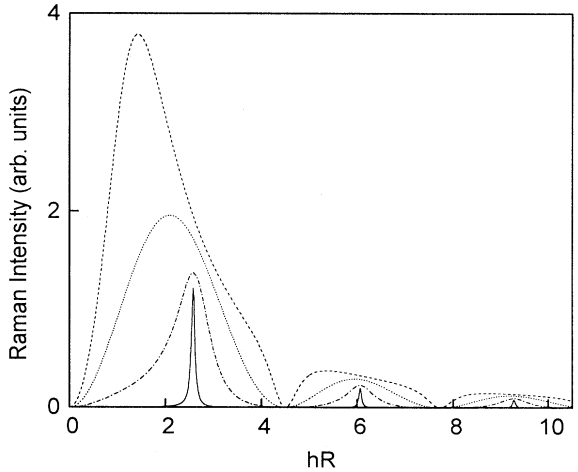

FIG. 3. Calculated Raman spectra of the $l = 0$ modes of a sphere of radius R, mass density ρ, and longitudinal and transverse sound velocities V_L and V_T embedded in an elastic medium with parameters $V_L/V_T = V_{Lm}/V_{Tm} = 3^{1/2}$. Solid line: $\rho_m/\rho = 0.05$; dotted dashed line: $\rho_m/\rho = 1/3$; dotted line: $\rho_m/\rho = 1$; dashed line: $\rho_m/\rho = 3$.

$$A^m_{\alpha\beta\gamma\delta}\int_V e^{i\mathbf{k}\cdot\mathbf{r}}dv \tag{35}$$

vanishes. The last integral is over the total volume of the sample, and its vanishing is equivalent to the well-known physical result that no Raman scattering is observed from acoustic phonons in crystals.[28] By integrating, Eq. (34) becomes

$$B^{\bar{k}}_{\alpha\beta} = \frac{i4\pi R^2}{\sqrt{V}}\sum_{\gamma\delta} e_{0\gamma}\frac{k_\delta}{k}\Delta A_{\alpha\beta\gamma\delta}\left(\frac{1}{(kR)^2}[\sin(kR) - kR\cos(kR)]\right), \tag{36}$$

which gives the amplitude of the wave scattered by the phonon with wave vector $\mathbf{k}$. The Raman spectrum is obtained by squaring Eq. (36) and summing over $\mathbf{k}$ and over the three polarization directions of the phonons. For each transversal or longitudinal phonon branch this can be done in two steps, first over the direction of propagation and of polarization of phonons, and then over the module of k. Since $\omega_l = V_L k$, and $\omega_t = V_T k$ in the low-frequency acoustic bands, the frequency spectrum is given by the k dependence of Eq. (36):

$$I^s_{\alpha\beta}(\omega = V_s k_s) \propto \frac{n+1}{\omega}\rho(\omega)\frac{1}{(k_s R)^4}[\sin(k_s R) - k_s R\cos(k_s R)]^2 \tag{37}$$

where the index s labels the contribution of transverse or longitudinal phonons. In the high-temperature limit, the frequency dependence of the term $(n+1)/\omega \simeq K_B T/(\hbar\omega^2)$ is balanced by that of the low-frequency density of states $\rho(\omega) \simeq \omega^2$. The spectrum given by Eq. (37) for longitudinal phonons coincides with that of Fig. 3(c), for $l = 0$ spheroidal modes in the absence of mechanical mismatch ($h = k_l$). In fact, in this case the $l = 0$ spheroidal modes with wave vector h are nothing but a symmetrical spherical wave packet of longitudinal phonons with $k_l = h$. The first, more intense peak occurs at $hR = 2.082$, to be compared with the values for the free sphere given by Fig. 1.

This study shows that the surrounding medium very much affects the shape of the Raman spectrum of a spherical particle. The discrete spectrum of the free particle is a good approximation only if the medium has a density (or sound velocity) much lower than that of the sphere. In general, one should be very careful in deducing the mean size of the particles from the energy position of the Raman peak and the size distribution from the linewidth. There are two sources of line broadening, an inhomogeneous one in the presence of a size distribution of particles, and a homogeneous one caused by the interaction of the particles with the surrounding medium.

Finally, we present the spectra calculated for two physical systems, which have been extensively studied by Raman scattering because of their interest for applications in nonlinear optics. Figure 4 shows the VV Raman spectrum of the symmetric modes calculated with the parameter suited for $CdS_{0.4}Se_{0.6}$ in silica glass ($\rho_m/\rho = 2.3/5.4$, $V_{Lm}/V_L = 5960/3850$, $V_L/V_T = 2.3$, $V_{Lm}/V_{Tm} = 5960/3790$).[10,29] For comparison, we also show the spectrum calculated for a quasifree particle, obtained with $\rho_m = \rho(SiO_2)/10$. For this system the matrix effect is quite important in broadening the Raman lines. We note that the experimental Raman spectra obtained by Champagnon, Andrianasolo, and Duval[10] and by Ferrari, Champagnon, and Barland[30] have a shape very similar to that in Fig. 4. This seems to indicate that most of the observed linewidth has a "homogeneous" origin. The width of the size distribution, obtained by assuming an inhomogeneous origin for the whole linewidth, is indeed overestimated.

Figure 5 shows the Raman spectrum calculated with parameters suited for Ag particles in silica glass ($\rho_m/\rho = 2.2/10.5$, $V_{Lm}/V_L = 5960/3650$, $V_L/V_T = 3650/1660$, $V_{Lm}/V_{Tm} = 5960/3790$).[12,29] The spectrum for a "quasifree" Ag sphere, obtained by putting $\rho_m = \rho(SiO_2)/10$, is again shown for comparison. In this case, the small shift and the small linewidth of the surface mode allow us to use with confidence the free-sphere model. We note that the calculations are performed for the $l = 0$ spectrum, but the experimental Ag spectrum is assigned to the $l = 2$ vibrations. However, in this case we expect that the matrix effect is small for all modes, and not only for the $l = 0$, because of the low $\rho(SiO_2)/\rho(Ag)$ ratio.

The two above examples suggest how one can obtain information on the size distribution from an experimental spectrum in the presence of both homogeneous and inhomogeneous broadening. One can try to fit the data

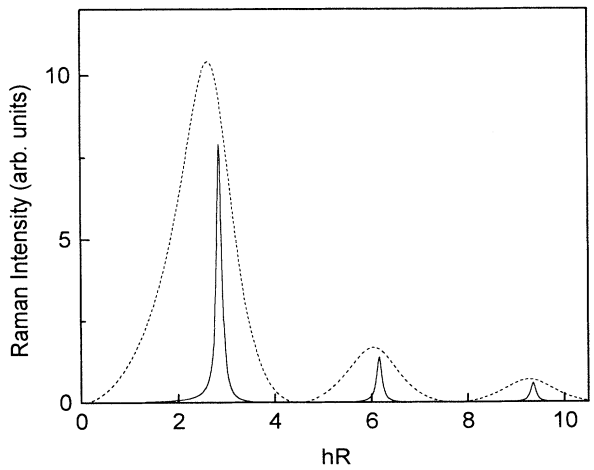

FIG. 4. Calculated Raman spectra of the $l = 0$ modes of a sphere of radius R of $CdS_{0.4}Se_{0.6}$ in silica glass (dashed line). The solid line is for $\rho_m = \rho(SiO_2)/10$ (see text).

by calculating the convolution of the homogeneous spectrum with a hypothesized size distribution (the quantity to be determined), and by taking as weights the Raman activities given by Eq. (24).

A complication can arise in the presence of electronic resonances. This is the case of both examples discussed above. The resonance with electronic excitations is very important because it strongly enhances the Raman signals but can cause size selection if the energies and wave functions of surface plasmons or excitons depend on the size of the particle. In this case, the line shape of the Raman peak depends on the excitation frequency, as observed in some systems.[2,18,26] However, this effect does not prevent the use of Raman scattering as a very simple and powerful tool for the determination of the sizes of nanoclusters.

VII. CONCLUSIONS

The Raman scattering from the acoustic vibrations of a small crystalline sphere can be obtained by calculating two sets of quantities. The first set consists of the mean components of the strain tensor relative to each vibrational mode. They are evaluated within a continuum approximation, which considers a vibrating homogeneous sphere. The second set are parameters related to the crystalline structure and to the physical mechanism of scattering and must be calculated for the system under study. The mean strains are different from zero only for the symmetric ($l = 0$) and the quadrupolar ($l = 2$) spheroidal vibrations, which are indeed the only Raman-active modes, as pointed out by Duval on the basis of symmetry arguments.[17] Symmetric vibrations cause polarized spectra; quadrupolar vibrations cause depolarized spectra with a depolarization ratio depending on the structure parameters. For cubic Bravais lattices and for the DID scattering mechanism, the symmetric vibrations are not Raman active, and the quadrupolar vibrations have a depolarization ratio of 1/3. The Raman activity of the surface modes and of a few low-frequency inner modes has been calculated for a particular value of the ratio between the mean longitudinal and transverse sound velocities, $V_L/V_T = \sqrt{3}$. Inner modes have quite low Raman activities with respect to surface modes.

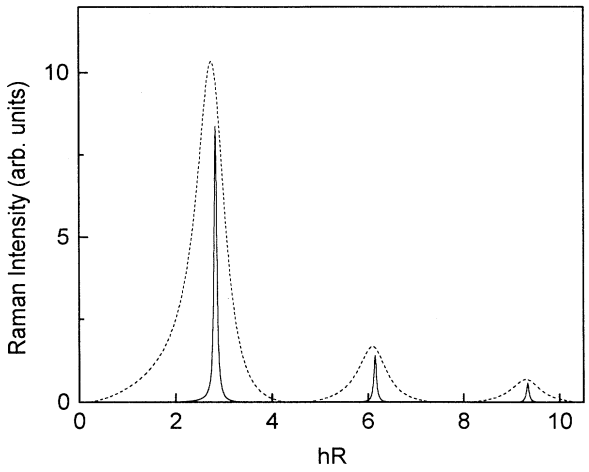

FIG. 5. Calculated Raman spectra of the $l = 0$ modes of a sphere of radius R of silver in silica glass (dashed line). The solid line is for $\rho_m = \rho(SiO_2)/10$ (see text).

The effect of a surrounding elastic medium has been taken into account. The discrete spectrum of a free sphere evolves into a continuum one as ρ_m/ρ increases. The homogeneous profile of the Raman spectrum must be taken into account when we deduce the particle size distribution. Resonance effects with electronic excitation and deviation from the spherical shape cause a partial loss of validity of the deduced laws.

New experimental data are needed to check the results of the present study. In particular, it would be very interesting to compare the Raman spectra of systems with a given distribution of particles embedded in different host media.

ACKNOWLEDGMENTS

The authors wish to express their appreciation to E. Duval, G. Ruocco, and G. Viliani for many helpful comments concerning this work.

[1] C. Flytzanis, F. Hache, M.C. Klein, D. Ricard, and Ph. Roussignol, *Progress in Optics XXIX*, edited by E. Wolf (Elsevier, Amsterdam, 1991), p. 322.
[2] D.A. Weitz, T.J. Gramila, A.Z. Genack, and J.I. Gersten, Phys. Rev. Lett. **45**, 355 (1980).
[3] E. Duval, A. Boukenter, and B. Champagnon, Phys. Rev. Lett. **56**, 2052 (1986).
[4] E. Rzepka, L. Taurel, and S. Lefrant, Surf. Sci. **106**, 345 (1981).
[5] G. Mariotto, M. Montagna, G. Viliani, E. Duval, S. Lefrant, E. Rzepka, and C. Mai, Europhys. Lett. **6**, 239 (1988).
[6] B. Champagnon, A. Boukenter, E. Duval, C. Mai, G. Vigier, and E. Rodek, J. Non-Cryst. Solids **94**, 216 (1987).
[7] H.B. Abel, Phys. Status Solidi B **161**, 435 (1990).
[8] A. Boukenter, B. Champagnon, E. Duval, J.L. Rousset, J. Dumas, and J. Serughetti, J. Phys. C **21**, L1097 (1988).
[9] V.K. Malinovsky, V.N. Novikov, A.P. Sokolov, and V.G. Dodonov, Solid State Commun. **67**, 725 (1988).
[10] B. Champagnon, B. Andrianasolo, and E. Duval, J. Chem. Phys. **94**, 5237 (1991).
[11] J.A. Capobianco, P.P. Proulx, B. Andrianasolo, and B. Champagnon, Phys. Rev. B **43**, 10 031 (1991).
[12] M. Fujii, T. Nagareda, S. Hayashi, and K. Yamamoto, Phys. Rev. B **44**, 6243 (1991).
[13] A. Tanaka, S. Onari, and T. Arai, Phys. Rev. B **47**, 1237 (1993).
[14] B. Champagnon, B. Andrianasolo, A. Ramos, M. Gandais,

M. Allais, and J.P. Benoit, J. Appl. Phys. **73**, 2775 (1993).
[15] H. Lamb, Proc. London Math. Soc. **13**, 187 (1882).
[16] A. Tamura, K. Higeta, and T. Ichinokawa, J. Phys. C **15**, 4975 (1982).
[17] E. Duval, Phys. Rev. B **46**, 5795 (1992).
[18] M. Ferrari, L.M. Gratton, A. Maddalena, M. Montagna, and C. Tosello, J. Non-Cryst. Solids (to be published).
[19] B.J. Berne and R. Pecora, *Dynamic Light Scattering* (Wiley, New York, 1976).
[20] P. Benassi, O. Pilla, V. Mazzacurati, M. Montagna, G. Ruocco, and G. Signorelli, Phys. Rev. B **44**, 11 734 (1991).
[21] V. Mazzacurati, M. Montagna, O. Pilla, G. Viliani, G. Ruocco, and G. Signorelli, Phys. Rev. B **45**, 2126 (1992).
[22] A.E.H. Love, *A Treatise on the Mathematical Theory of Elasticity* (Dover, New York, 1944).
[23] A.C. Eringen and E.S. Suhubi, in *Elastodynamics* (Academic, New York, 1975), Vol. II.
[24] N. Nishiguchi and T. Sakuma, Solid State Commun. **38**, 1073 (1981).
[25] V. Mazzacurati and G. Ruocco, Mol. Phys. **61**, 1391 (1987).
[26] E. Duval, G. Mariotto, M. Montagna, O. Pilla , G. Viliani, and M. Barland, Europhys. Lett. **3**, 333 (1987).
[27] M. Barland, E. Duval, C. Mai, G. Mariotto, M. Montagna, and G. Viliani, Physica A **157**, 539 (1989).
[28] We are considering nanoparticles with $qR \ll 1$, where q is the exchanged wave vector of the light. The term $e^{i\mathbf{q}\cdot\mathbf{r}}$ has been neglected in Eqs. (17), and (33), and this means that we do not consider the Brillouin scattering. This occurs for $\mathbf{k} = \mathbf{q}$, at frequencies lower than those of Raman scattering, which occurs for $kR \simeq 1$.
[29] D. Heiman, D.S. Hamilton, and R.W. Hellwarth, Phys. Rev. B **19**, 6583 (1979).
[30] M. Ferrari, B. Champagnon, and M. Barland, J. Non-Cryst. Solids **151**, 95 (1992).